Published in final edited form as:

Cell Rep. 2022 July 12; 40(2): 111072. doi:10.1016/j.celrep.2022.111072.

Autism-associated chromatin remodeler CHD8 regulates erythroblast cytokinesis and fine-tunes the balance of Rho GTPase signaling

Zhaowei Tu[1,2], **Cuiqing Fan**[2], **Ashely K. Davis**[2], **Mengwen Hu**[3], **Chen Wang**[2], **Akhila Dandamudi**[2], **Katie G. Seu**[2], **Theodosia A. Kalfa**[2], **Q. Richard Lu**[2], **Yi Zheng**[2,4,*]

[1]Department of Obstetrics and Gynecology, Guangdong Provincial Key Laboratory for Major Obstetric Diseases, Guangdong Engineering and Technology Research Center of Maternal-Fetal Medicine, Guangdong-Hong Kong-Macao Greater Bay Area Higher Education Joint Laboratory of Maternal-Fetal Medicine, The Third Affiliated Hospital of Guangzhou Medical University, Guangzhou 510150, China

[2]Cancer and Blood Diseases Institute, Cincinnati Children's Hospital Medical Center, University of Cincinnati College of Medicine, 3333 Burnet Avenue, Cincinnati, OH 45229, USA

[3]Department of Microbiology and Molecular Genetics, University of California, Davis, Davis, CA, USA

[4]Lead contact

SUMMARY

CHD8 is an ATP-dependent chromatin-remodeling factor whose monoallelic mutation defines a subtype of autism spectrum disorders (ASDs). Previous work found that CHD8 is required for the maintenance of hematopoiesis by integrating ATM-P53-mediated survival of hematopoietic stem/progenitor cells (HSPCs). Here, by using *Chd8*$^{F/F}$*Mx1-Cre* combined with a *Trp53*$^{F/F}$ mouse model that suppresses apoptosis of *Chd8*$^{-/-}$ HSPCs, we identify CHD8 as an essential regulator of erythroid differentiation. *Chd8*$^{-/-}$ *P53*$^{-/-}$ mice exhibited severe anemia conforming to congenital dyserythropoietic anemia (CDA) phenotypes. Loss of CHD8 leads to drastically decreased numbers of orthochromatic erythroblasts and increased binucleated and multinucleated basophilic erythroblasts with a cytokinesis failure in erythroblasts. CHD8 binds directly to the gene bodies of multiple Rho GTPase signaling genes in erythroblasts, and loss of CHD8 results in their dysregulated expression, leading to decreased RhoA and increased Rac1 and Cdc42 activities. Our study shows that autism-associated CHD8 is essential for erythroblast cytokinesis.

*Correspondence: yi.zheng@cchmc.org.

AUTHOR CONTRIBUTIONS

Z.T., Q.R.L., and Y.Z. designed the study. Z.T. performed experiments, interpreted data, and generated the figures. C.F., A.K.D., C.W., M.H., and A.D. performed experiments. K.G.S. and T.A.K. interpreted data. Z.T. and Y.Z. wrote manuscript. Y.Z. provided funding support.

SUPPLEMENTAL INFORMATION

Supplemental information can be found online at https://doi.org/10.1016/j.celrep.2022.111072.

DECLARATION OF INTERESTS

The authors declare no competing financial interests.

Author Manuscript

Author Manuscript

Author Manuscript

Graphical Abstract

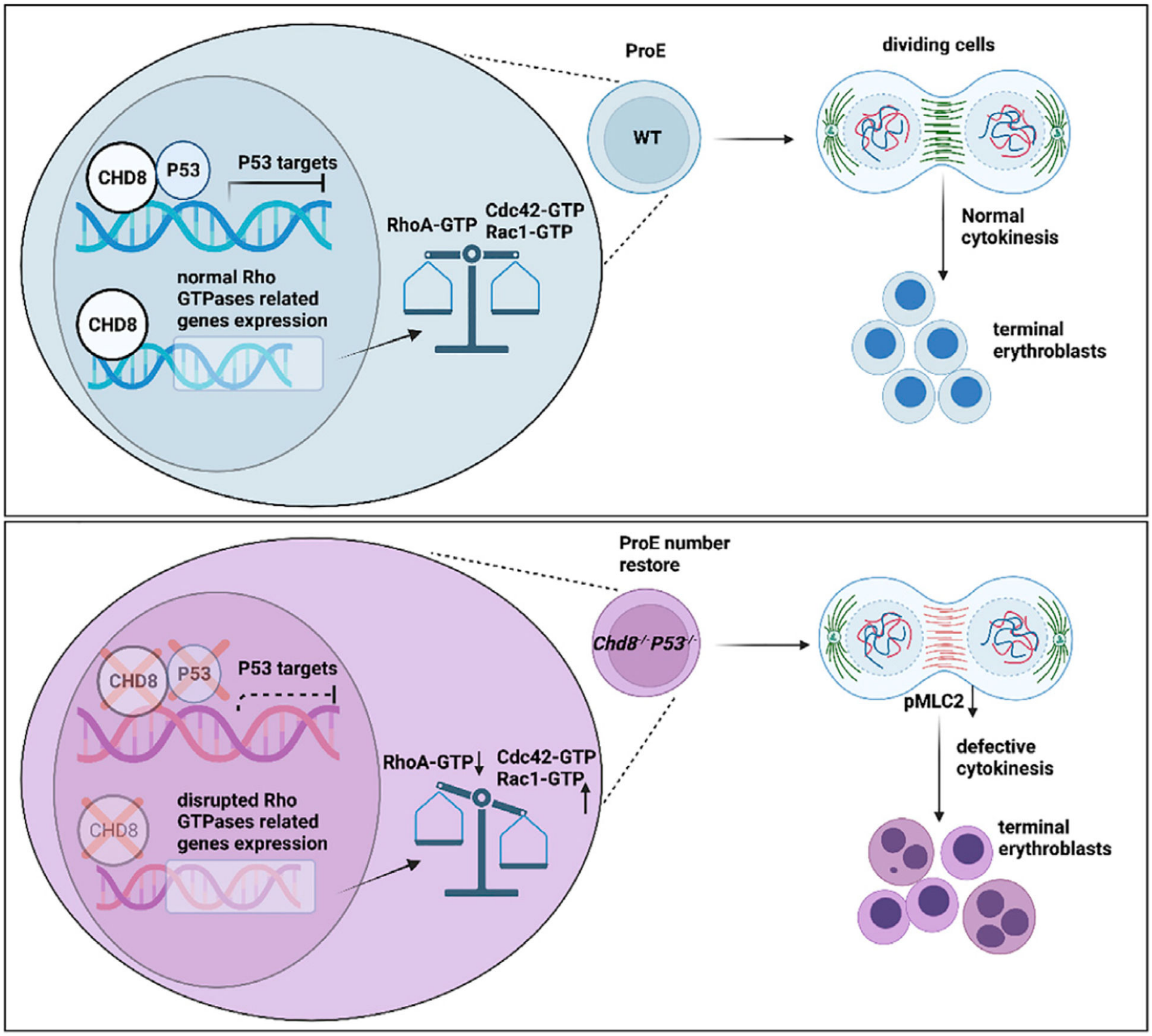

In brief

Tu et al. report that CHD8, an autism-related chromatin remodeler, is essential for erythroid differentiation. Loss of CHD8 leads to unbalanced Rho GTPase signaling and defective erythroblast cytokinesis, mimicking that of congenital dyserythropoietic anemia.

INTRODUCTION

During erythropoiesis, proerythroblasts undergo 3–4 cell divisions to generate orthochromatic erythroblasts (OrthoEs). In this course, nuclear condensation is coupled with differentiation, which is completed by extrusion of the nucleus to form a reticulocyte (Ji et al., 2011; Menon and Ghaffari, 2021). Histone modification and epigenetic regulation, vesicle trafficking, transcriptional regulation, cytoskeleton remodeling, and cytokinesis are required events (Mei et al., 2021).

Rho GTPases integrate a variety of signals involved in cytoskeleton arrangement, microtubule dynamics, vesicular transport pathways, and gene expression, as well as cell-cycle progression (Etienne-Manneville and Hall, 2002; Jaffe and Hall, 2005). They are essential for erythroid development (Kalfa and Zheng, 2014). Loss of RhoA or its target mDia2 leads to erythroblast cytokinesis failure (Konstantinidis et al., 2015; Mei et al., 2016; Watanabe et al., 2013), whereas disruption of Rac1 and Rac2 GTPase activities inhibits enucleation (Ji et al., 2008; Konstantinidis et al., 2012). Cdc42 also plays an important role in cytokinesis, nuclear polarization, and nuclear extrusion during erythroblast differentiation (Ubukawa et al., 2020). Recent studies have found that a precise balance of the activities of Rho GTPases, maintained by *RACGAP1*, is required for erythroblast cytokinesis, the disruption of which can be causal for a subtype of congenital dyserythropoietic anemia, CDA III (Romero-Cortadellas et al., 2021; Wontakal et al., 2022).

ATP-dependent chromatin remodelers are essential in erythroid cells. Brg1 is required for β-globin regulation and erythropoiesis *in vivo*, while CHD4 mediates silencing of fetal globin gene in adult erythroid cells (Amaya et al., 2013; Bultman et al., 2005). BRG1/BRM-associated factor (BAF)-mediated chromatin remodeling at the erythromyeloid progenitor stage is critical for myeloid and definitive erythroid lineage development (Wu et al., 2020). Chromodomain helicase DNA-binding protein 8 (CHD8) is an ATP-dependent chromatin-remodeling factor whose mutations have been associated with autism spectrum disorders (Bernier et al., 2014; Katayama et al., 2016). Besides its well-known functions of restricting P53 and β-catenin signaling through histone H1 binding, CHD8 is also critical in transcription regulation in neural progenitors and oligodendrocytes (Durak et al., 2016; Nishiyama et al., 2009; Sood et al., 2020; Thompson et al., 2008; Zhao et al., 2018). We and others have demonstrated recently that CHD8 is essential for hematopoietic stem/progenitor cell (HSPC) maintenance by restricting P53 signaling (Nita et al., 2021; Tu et al., 2021).

Here, by using the *Chd8*$^{F/F}$*Mx1-Cre* combined with *Trp53*$^{F/F}$ mouse model, we found that P53 deletion could restore white blood cell (WBC) counts in peripheral blood but not red blood cell (RBC) or hemoglobin (Hb) levels upon CHD8 depletion. *Chd8*$^{-/-}$ *P53*$^{-/-}$ mice died of severe anemia, attributable to defects in erythroid differentiation due to failure of erythroblast cytokinesis, mimicking that of congenital dyserythropoietic anemia (CDA) phenotypes. CHD8 binds directly to the gene bodies of multiple Rho GTPase signaling genes in erythroblasts, and loss of CHD8 results in their dysregulated expression, leading to decreased RhoA and increased Rac1 and Cdc42 activities. Our study implicates CHD8 as an essential factor in immature erythroblast cytokinesis related to CDA-like phenotypes.

RESULTS

Chd8$^{-/-}$ *P53*$^{-/-}$ mice suffer severe anemia due to loss of erythroid precursors in the bone marrow (BM)

Previous studies have revealed a significant role of CHD8 in HSPC maintenance through restricting P53 signaling and loss of P53 restored HSPC survival (Nita et al., 2021; Tu et al., 2021). However, the role of CHD8 in mature hematopoietic cell differentiation and whether conditional P53 deletion rescues all the defects caused by CHD8 loss remain unclear. We have performed tracing of peripheral blood counts at different times in wild-type (WT), *P53*$^{-/-}$, and *Chd8*$^{-/-}$ *P53*$^{-/-}$ mice after pI:pC injection. In erythroblasts, CHD8 and P53 are efficiently deleted after pI:pC induction (Figure 1A). The anemia phenotype we previously described to be caused by CHD8 deletion, as evidenced by decreasing RBC count, Hb, and hematocrit (Hct) values, could not be rescued by P53 deletion (Figure 1B), while WBC counts were restored (Figure S1A). Beginning from 1 week post-deletion, the anemia worsened over time, and C*hd8*$^{-/-}$ *P53*$^{-/-}$ mice did not survive past 120 days post pI:pC injection due to severe anemia (Figures 1B and S1B).

Next, we harvested BM at 2 weeks post-deletion, when *Chd8*$^{-/-}$ *P53*$^{-/-}$ mice already showed a phenotype in RBCs. Flow analysis of erythroid marker TER119 demonstrated that the ratio of TER119^{+} nucleated cells in *Chd8*$^{-/-}$ *P53*$^{-/-}$ BM was drastically decreased compared with *P53*$^{-/-}$ mice (Figure 1C). Furthermore, stained cytospins of *Chd8*$^{-/-}$ *P53*$^{-/-}$ BM cells showed a decrease in mature erythroid precursors and an increaseof binucleated erythroblasts (Figure 1D). These results indicate that CHD8 is required for steady-state erythropoiesis in BM.

Chd8$^{-/-}$ *P53*$^{-/-}$ erythroid progenitors are defective in colony-forming activity

The process of erythropoiesis starts with the multipotent hematopoietic stem cell. Previously, we found that loss of CHD8 caused depletion of megakaryocyte erythroid progenitors (MEPs; CD34^{-}FcgR^{low}) and that additional P53 knockout restored the MEP number (Tu et al., 2021). Here, using another well-defined flow cytometry method with markers CD41, CD150, and endoglin (Pronk et al., 2007), we observed decreased numbers of preMegE, preCFU-E, CFU-E + proEry, and MkP in *Chd8*$^{-/-}$ BM, while *Chd8*$^{-/-}$ *P53*$^{-/-}$ mice had more of these progenitors than *P53*$^{-/-}$ mice (Figure S1C), suggesting that the anemia phenotype in *Chd8*$^{-/-}$ *P53*$^{-/-}$ mice was not due to reduced erythroid progenitors in the BM. We further performed burst-forming unit erythroid (BFU-E) and colony-forming unit erythroid (CFU-E) assays. The BFU-E colonies formed from *Chd8*$^{-/-}$ *P53*$^{-/-}$ cells were smaller than those generated from *P53*$^{-/-}$ BM cells; *Chd8*$^{-/-}$ *P53*$^{-/-}$ cells also produced fewer CFU-Es and BFU-Es (Figures S1D and S1E). These results indicate that CHD8 regulation of erythropoiesis may be at the erythroblast differentiation stage.

CHD8 is essential for erythropoiesis in the BM

To examine whether CHD8 plays a role in erythroid differentiation, we performed flow cytometry of the BM utilizing CD44, TER119, and size (forward scatter) to separate the erythroid cells into proerythroblasts (ProEs), basophilic erythroblasts (BasoEs), polychromatic erythroblasts (PolyEs), OrthoEs, and reticulocytes (Retics) (Liu et al., 2013). As shown in Figure 1E, deletion of CHD8 led to significant loss of erythroblasts compared with WT mice. Loss of P53 in *Chd8*$^{-/-}$ mice restored the number of erythroid progenitors, but erythroblast differentiation remained impaired. We observed a severely decreased number of late erythroblasts (OrthoEs) in the BM of *Chd8*$^{-/-}$ *P53*$^{-/-}$ mice, while there were significantly more ProE cells (Figure 1F), supporting that CHD8 is essential for steady-state erythroblast differentiation in the BM.

In addition, we performed non-competitive transplantation and observed erythropoiesis in the transplanted CD45.1 recipients (Figure S1F). While deletion of P53 in *Chd8*$^{-/-}$ cells improved their survival, the mice all died before 50 days post-transplantation (Figure S1G). Peripheral blood counts at 4 weeks post-transplantation showed that WT recipients engrafted with *Chd8*$^{-/-}$ *P53*$^{-/-}$ BM experienced critical anemia, with RBC, Hb, and Hct counts notably decreased as in *Chd8*$^{-/-}$ *P53*$^{-/-}$ mice and with no obvious changes in WBC and platelet (PLT) counts (Figure S1H). Flow cytometry of erythroblasts analyzed as per CD71 and TER119 also showed increased late erythroid progenitors and decreased mature erythroblasts after loss of CHD8 in the *P53*$^{-/-}$ background (Figures S1I and S1J). These results from transplanted recipients demonstrate an erythroblast intrinsic role of CHD8 in erythropoiesis, crucial for differentiation after the BasoE stage.

Loss of CHD8 in the *P53*$^{-/-}$ background led to extensive extramedullary erythropoiesis

Ineffective erythroblast differentiation in the BM could activate extramedullary stress erythropoiesis. Firstly, we measured serum erythropoietin (EPO) levels at 2 weeks post CHD8 deletion and found that EPO increased more than 100-fold in *Chd8*$^{-/-}$ *P53*$^{-/-}$ mice (Figure S2A). Secondly, *Chd8*$^{-/-}$ *P53*$^{-/-}$ mice showed splenomegaly and increased spleen cellularity (Figures S2B and S2C). Flow analysis revealed increased total counts of TER119^{+} cells in *Chd8*$^{-/-}$ *P53*$^{-/-}$ spleen (Figure S2D). However, dysplastic erythroblasts were still observed in cytospins of the spleen cells, which were absent in WT and *P53*$^{-/-}$ spleens (Figure S2E), suggesting defective splenic erythropoiesis. To further test this, we harvested spleen cells at 2 weeks post pI:pC injection and performed flow cytometry. As described in the BM, we saw an increased ratio of cells in the ProE (WT, 0.1157%; *P53*$^{-/-}$, 0.1170%; *Chd8*$^{-/-}$ *P53*$^{-/-}$, 1.990%) and BasoE (WT, 0.5467%; *P53*$^{-/-}$, 0.46%; *Chd8*$^{-/-}$ *P53*$^{-/-}$, 3.783%) populations but decreased or unchanged frequencies of OrthoE (WT, 2.85%; *P53*$^{-/-}$, 1.933%; *Chd8*$^{-/-}$ *P53*$^{-/-}$, 2.633%) and retic (WT, 14.07%; *P53*$^{-/-}$, 15.7%; *Chd8*$^{-/-}$ *P53*$^{-/-}$, 7.777%) out of the TER119^{+} population (Figures S2F and S2G). Total cell count confirmed this change (Figure S2H). These results indicate that CHD8 is required not only for BM erythropoiesis but also for extramedullary stress erythropoiesis in the spleen.

CHD8 is required for erythroblast cytokinesis

To determine the cause of ineffective erythroid differentiation, we checked the cell death of late erythroblasts with annexin V and did not detect significant increased apoptosis *in vivo* or *ex vivo* in *Chd8*$^{-/-}$ *P53*$^{-/-}$ cells (Figure S3A). We analyzed the cell cycle of erythroblasts using 5-Bromo-2′-deoxyuridine (BrdU) incorporation assay and observed a dramatic increase in G2/M phase as well as an increased number of polyploid erythroblasts (>4N) from *Chd8*$^{-/-}$ *P53*$^{-/-}$ mice beginning with ProEs and becoming more pronounced in the TER119^{+} population (Figures 2A–2C). In TER119^{+} cells, the increase in G2/M and >4N cells was accompanied by a significant decrease in G0/G1 and S phases in *Chd8*$^{-/-}$ *P53*$^{-/-}$ mice (Figure 2C). Similar results were obtained by propidium iodide (PI) staining of BM cells after CHD8 loss (Figures S3B and S3C). These results suggest that CHD8 is required for normal cell division of erythroblasts. Moreover, we sorted ProE and BasoE + PolyE from WT, *P53*$^{-/-}$, and *Chd8*$^{-/-}$ *P53*$^{-/-}$ BM using CD44 and TER119 markers and performed Wright staining of these cells. Consistent with the BrdU and PI flow results, we found more biand multi-nucleated *Chd8*$^{-/-}$ *P53*$^{-/-}$ BasoEs and PolyEs (Figure 2D). We also observed bi- and multi-nucleated cells in the *Chd8*$^{-/-}$ *P53*$^{-/-}$ ProE population, but they were not as frequent as in the BasoEs + PolyEs. PI staining of sorted BasoE + PolyE cells revealed that more than 10% *Chd8*$^{-/-}$ *P53*$^{-/-}$ cells were in >4N phase (Figure 2E). *Chd8*$^{-/-}$ *P53*$^{-/-}$ CD71^{+}TER119^{+} erythroblasts also contained a significantly increased amount of >4N cells, and multi-nucleated erythroblasts could be easily found in the sorted *Chd8*$^{-/-}$ *P53*$^{-/-}$ CD71^{+}TER119^{+} population (Figures S3D and S3E).

In addition to the BM, we also analyzed the cell cycle of spleen erythroblasts by flow cytometry. As in the BM, we detected more TER119^{+} cells in 2N–4N, 4N, and >4N and less cells in the 2N phase, indicating retarded cell-cycle progression and cytokinesis failure (Figure 2F). These results show that CHD8 is essential for erythroblast cytokinesis during differentiation in both BM and spleen. Together, the phenotypes of CHD8 loss mimic that of CDA (Iolascon et al., 2013, 2020).

CHD8 balances Rho GTPase signaling in erythroblasts by controlling gene expression

To elucidate the underlying mechanism of disturbed cytokinesis in *Chd8*$^{-/-}$ *P53*$^{-/-}$ erythroblasts, we sorted ProEs from different genotypes and performed RNA sequencing at 2 weeks postdeletion. Principal-component analysis (PCA) confirmed that the replicates of each genotype were well correlated (Figure 3A). We found 2,206 differentially expressed genes (DEGs) between *Chd8*$^{-/-}$ *P53*$^{-/-}$ and WT cells and 2,375 DEGs between *Chd8*$^{-/-}$ *P53*$^{-/-}$ and *P53*$^{-/-}$ cells (Figure 3B). Next, we overlapped the up- and down-regulated transcripts between the two comparisons and found 793 commonly up-regulated genes and 932 down-regulated genes, which account for the majority of the DEGs (Figure 3C). The expression level of key factors in erythropoiesis showed increased *Gata1* and decreased *Stat5a* levels in *Chd8*$^{-/-}$ *P53*$^{-/-}$ cells, while *Klf1* was not changed (Figure 3D). RT-PCR of sorted erythroblasts from BM further confirmed these changes (Figure 3E), suggesting that the cytokinesis failure was not due to down-regulated expression of GATA1 and KLF1. Next, we performed Gene Ontology (GO) pathway enrichment with the overlapping DEGs as previously reported (Zhou et al., 2019). The genes involved in actin cytoskeleton organization and Rho GTPase signaling were highly enriched (Figure 3F), whereas conventional CHD8-regulated β-catenin signaling (Nishiyama et al., 2012; Thompson et al., 2008) was not changed (Figures S4A and S4B). Further western blotting of erythroblasts confirmed the altered protein expression of Rho GTPase signaling such as RHOF, LBR, ARHGAP11A, PAK6, and LIMK1 (Figure S4C). These results suggest that CHD8 may regulate erythroblast cytokinesis by disrupting gene expression related to Rho signaling.

To further test this hypothesis, we sorted WT CD45^{-} CD44^{+}TER119^{+} erythroblasts and performed CHD8 CUT&RUN assay to define its potential targets. The peaks were called with Sparse Enrichment Analysis for CUT&RUN (SEACR) stringent mode, showing that CHD8 binding peaks were primarily localized on the gene body region, including introns, transcription start sites (TSSs), and exons (Figure 4A). GO analysis of CHD8 binding genes showed top enrichment in cell-cycle and chromatin-organization pathways (Figures S4D and S4E). Subsequently, we overlapped CHD8 binding genes found in CUT&RUN assay with

DEGs of *Chd8*$^{-/-}$ *P53*$^{-/-}$ cells found in RNA sequencing (RNA-seq) data. In total, there were 810 genes identified that were potential CHD8 direct targets (Figure 4B). As shown in GO analysis of DEGs in the RNA-seq data, the "signaling by Rho GTPases" pathway was enriched in CHD8 direct targets (Figure 4C). Indeed, we can see direct binding of CHD8 on the promoter of Rho-signaling-related genes like *Rhof*, *Arfgap3*, *Arhgap11a*, *Pak6*, and *Arpc2* (Figure 4D). In these Rho-signaling-related targets, there were 26 genes increased including *Arhgap11a*, *Cdc42ep3*, *Rhof*, *Pak6*, and *Vangl1* and 19 genes including *Arhgap45*, *Arfgap3*, *Arpc2*, *limk1*, and *Dync1i2* decreased in *Chd8*$^{-/-}$ *P53*$^{-/-}$ erythroblasts (Figure 4E). These results suggest that CHD8 is essential for fine-tuning Rho signaling gene expression in immature erythroblasts.

The Rho GTPase effector domain pull-down assay has been widely used for probing the respective active Rho-GTP levels in cells (Jennings and Knaus, 2014). We further performed this assay with immobilized GST-Rhotekin or -PAK to detect RhoA-GTP, Rac1-GTP, and Cdc42-GTP in CD45^{-}TER119^{+} BM cells. We observed decreased RhoA-GTP levels but increased Rac1-GTP and Cdc42-GTP levels in *Chd8*$^{-/-}$ *P53*$^{-/-}$ cells (Figures 4F and 4G), indicating altered Rho GTPase signaling due to loss of CHD8. RhoA inactivation could affect myosin light chain 2 (MLC2 Ser19) activity and lead to cytokinesis failure (Konstantinidis et al., 2015), and the pMLC2 level was significantly down-regulated in *Chd8*$^{-/-}$ *P53*$^{-/-}$ cells (Figure 4F). Thus, CHD8 appears to maintain a balance of Rho GTPase signaling genes essential for erythroblast cytokinesis. Interestingly, such a mechanism of erythroblast regulation mimics that reported recently for CDA III patients (Romero-Cortadellas et al., 2021; Wontakal et al., 2022).

DISCUSSION

We and others have reported that CHD8 is required for HSPC survival by restricting P53 signaling activation. Loss of P53 could restore the survival of *Chd8*$^{-/-}$ HSPCs (Nita et al., 2021; Tu et al., 2021). Here, we found that loss of CHD8 in the *P53*$^{-/-}$ background led to erythroblast cytokinesis defects and accumulation of bi- and multi-nucleated cells resulting in decreased number of erythroblasts without a significant effect on myeloid or lymphoid development. Mechanistically, CHD8 binds to the gene body of Rho signaling genes and controls their expression to govern the balance of Rho GTPases activities, playing an essential role in erythropoiesis by a mechanism differing from previously established function in P53 and β-catenin-mediated signaling (Nishiyama et al., 2009, 2012; Tu et al., 2021). The study raises a possibility that CHD8-regulated erythroblast differentiation is involved in CDA (Iolascon et al., 2020) or in anemia of CHD8-associated autism in this underexplored area of studies (Yang et al., 2021).

Erythroid lineage sustains a rapid proliferation rate that requires successful erythroid cell division and separation. In mice, well-known factors involved in erythroblasts cytokinesis include RhoA and its effector mDia2; loss of either causes cytokinesis failure and ineffective erythropoiesis (Konstantinidis et al., 2015; Mei et al., 2016; Watanabe et al., 2013). We observed similar cytokinesis defects in *Chd8*$^{-/-}$ *P53*$^{-/-}$ cells and found that disrupted Rho signaling was involved. In humans, bi- and multi-nucleated erythroblasts are associated with CDA caused by mutations in several genes, including *CDAN1*, *CDIN1*, *SEC23B*, *KIF23*, *GATA1*, and *KLF1* (Iolascon et al., 2020). Two recent studies identified *RACGAP1* mutations resulting in unbalanced Rho GTPase activities and CDA III subtype (Romero-Cortadellas et al., 2021; Wontakal et al., 2022). Our findings suggest that loss of CHD8 leads to a CDA-like phenotype associated with dysregulation of Rho signaling.

As a chromatin remodeler, CHD8 has been found to be essential in transcriptional regulation in different cell types (Durak et al., 2016; Kita et al., 2018; Rodriguez-Paredes et al., 2009; Subtil-Rodriguez et al., 2014; Zhao et al., 2018). In $Chd8^{-/-}$ $P53^{-/-}$ erythroblasts, we detected multiple differentially expressed Rho GTPase signaling genes that affect the balanced Rho GTPase activities. Moreover, CUT&RUN assay in erythroblasts identified multiple Rho signaling genes as direct targets of CHD8, revealing a mechanism of CHD8 different from that in HSPCs or other tissues (Nita et al., 2021; Tu et al., 2021; Zhao et al., 2018). However, how CHD8 is recruited to its targets remain poorly understood. As a member of the CHD family, CHD8 protein contains double chromodomains that could directly bind to methylated lysines on histone H3 tails and nucleosomal DNA (Flanagan et al., 2005; Manning and Yusufzai, 2017). Further investigation is required to understand if erythroblasts may adopt such mechanisms.

In both mouse and human, loss or mutations of CHD8 is known to lead to neurodevelopmental disorders (Bernier et al., 2014; Durak et al., 2016; Kawamura et al., 2021; Kweon et al., 2021; Zhao et al., 2018). A recent paper found a significant association between anemia and neurodevelopmental disorders including autism spectrum disorder (ASD), attention-deficient/hyperactivity disorder (ADHD), and learning disability in a United States cohort (Yang et al., 2021), but no information is available for the underlying mechanism of such anemia beyond diseaserelated behaviors affecting nutritional intake. Our current work shows that CHD8 is essential for erythropoiesis and that CHD8 loss causes CDA III-like phenotypes in mice, raising the question of whether CHD8-related neurodevelopmental disorders are associated with erythropoiesis defects in patients with ASD.

Limitations of the study

Due to the essential role of P53 in CHD8-mediated blood stem/progenitor cell survival, compounding P53 deletion is needed to observe the erythroblast defects caused by CHD8 deletion. Furthermore, although our studies demonstrate a close association of CHD8 with the expression of Rho signaling genes/proteins and CHD8 binding to these gene bodies in erythroblasts, causal evidence that loss of CHD8 leads to erythroblast cytokinesis failure through a defined Rho signaling pathway is difficult to come by because of the involvement of multiple Rho signaling components.

STAR★METHODS

RESOURCE AVAILABILITY

Lead contact—Further information and requests for resources and reagents should be directed to and will be fulfilled by the lead contact, Yi Zheng (Yi.Zheng@cchmc.org)

Materials availability—This study did not generate new unique reagents.

Data and code availability

- The RNA-seq and CUT&RUN data have been deposited at the Gene Expression Omnibus (GEO) with accession code GSE189853 listed in the key resources table and are publicly available as of the date of publication. Original western blot images and microscopy data reported in this paper will be shared by the lead contact upon request.
- This paper does not report original code.
- Any additional information required to reanalyze the data reported in this paper is available from the lead contact upon request.

EXPERIMENTAL MODEL AND SUBJECT DETAILS

Animals—*Chd8^{Flox}* mice and *P53^{Flox}* mice were used as previously reported (Tu et al., 2021). To induce hematopoietic cell specific deletion, *Chd8^{Flox}* and *P53^{Flox}* mice were crossed with *Mx1-Cre* mice and injected with pI:pC (15mg/kg, GE healthcare) for 4 times and bone marrow cells were harvested at two weeks after last injection. 6 to 8 week old mice were used and the sex of the mice was not distinguished. After pI:pC injection, the *Chd8$^{F/F}$P53$^{F/F}$* mice were considered as WT, *Chd8$^{F/F}$Mx1-Cre* mice were considered as *Chd8$^{-/-}$*, *P53$^{F/F}$Mx1-Cre* mice were considered as *P53$^{-/-}$* and *Chd8$^{F/F}$P53$^{F/F}$ Mx1-Cre* mice were considered as *Chd8$^{-/-}$ P53$^{-/-}$*. All animal work was done in accordance with the protocols from the Institutional Animal Care and Use Committee at Cincinnati Children's Hospital Medical Center.

METHOD DETAILS

Blood cell count—Whole blood was collected from the superficial facial vein of the animals into EDTA-treated tubes at different time points after deletion induction. The total blood cell and differential counts were evaluated using a hematology analyzer (HEMAVET 950FS, Drew Scientific). The total bone marrow cellularity and spleen cellularity were also determined by the same machine.

Histology—Mouse spleens were harvested and fixed in 10% neutral buffered formalin, washed with PBS, and dehydrated in 70% ethanol. Paraffin embedding, sectioning, and staining with hematoxylin and eosin were performed by the Research Pathology Core at Cincinnati Children's Hospital Medical Center. BM and spleen cell cytospins were stained with CAMCO stain PAK (#702, Cambridge Diagnostic Products) and sorted erythroblast cytospins were stained with Wright solution (#740–75, Sigma).

Flow cytometry and cell sorting—Bone marrow cells were immunostained and analyzed on an LSRII flow cytometer (BD Biosciences). Fluorochrome-conjugated anti-mouse Ter119, CD45, CD44, CD71, CD117/c-Kit, Sca1, CD150, CD48, CD105, CD41 and CD16/32 antibodies were purchased from Biolegend. Cell death and apoptosis were analyzed using Annexin V (Biolegend, #640906) and DAPI (Thermo Fisher, D1306). For PI staining, bone marrow cells were stained with surface markers and then fixed with 70% ethanol for 15 min. Cells were washed and treated with RNase A (10ug/mL) at 37°C for

15 min. A final concentration of 50ug/mL PI were administered and cells were analyzed by flow.

To isolate erythroblasts, CD45 cells depletion was performed (CD45 MicroBeads, Miltenyi Biotec) and CD45-negative cells were then stained with CD45, TER119 and CD44 and sorted using a BD FACS Aria I or a BD FACS Aria III (BD bioscience)

Serum EPO level detection—The serum was collected from mice of different genotypes at 2 weeks after gene deletion and Mouse Erythropoietin ELISA Kit (Abcam, ab270893) was used for EPO level detection. Each sample were assayed with two replicates and the OD was recorded at 450nm as endpoint reading.

Colony forming—Methocult SF M3436 and Methocult M3334 medium were used to assay the colony forming ability of BFU-E and CFU-E separately. In brief, 5×10^4 cells per 1mL medium for BFU-E and 1×10^5 per 1 mL medium for CFU-E were seeded in triplicates and cultured in a humidified 37°C, 5%CO_2. CFU-E were scored 2 days after plating and BFU-E were scored 10 days after plating using an inverted microscope.

Bone marrow transplantation—For transplantation, a total of 2×10^6 fresh isolated bone marrow cells from WT, *Chd8*$^{-/-}$, *P53*$^{-/-}$ and *Chd8*$^{-/-}$ *P53*$^{-/-}$ mice were transplanted into lethally irradiated BoyJ mice (CD45.1). Peripheral blood and bone marrow were analyzed at different time points after transplantation.

BrdU labeling and staining—Bromodeoxyuridine (BrdU, Sigma) was made as 10mg/mL solution in PBS. The mice were weighted and injected with a dose of 1mg Brdu/6g body weight at 1 h before harvesting. The staining was done by the FITC BrdU Flow kit (Biosciences, #559619).

Western Blot—Whole bone marrow cells were lysed with RBC lysis buffer, followed by CD45$^+$ cell depletion using CD45 MicroBeads (Miltenyi Biotec, # 130-052-301) and Ter119$^+$ cells enrichment with Anti-Ter-119 MicroBeads (Miltenyi Biotec, #130-049-901). Ter119$^+$ cells were lysed and protein concentration was determined by Quick Start Bradford 1x Dye Reagent (Bio-rad, #5000205). For Western blot, Proteins were boiled in 4x Laemmli Sample Buffer (Bio-rad, #1610747) and same amount proteins were separated on a 4–15% TGX gel (BioRad, #1610377) and transferred to a PVDF membrane. The membranes were incubated with specific antibodies and bands were imaged using a BioRad ChemiDoc imager. The antibodies include pMLC2, MLC2, β-actin.

Rho-GTPases pull-down assay—GTPases pull-down assays were performed as previously reported (Shang et al., 2012). In briefly, same amount proteins of different genotypes were incubated with PAK beads for Rac1-GTP, Cdc42-GTP detection and Rhotekin beads for RhoA-GTP detection at 4°C. The beads were washed for 3 times and boiled in 40μL 2X Laemmli Sample Buffer. Same volume of pulldown samples was loaded in 4–15% TGX gel (BioRad, #1610377) and further blotted with anti-RhoA, anti-Rac1, anti-Cdc42 and β-actin.

RNA-seq—RNA was extracted from sorted proE cells. RNA-seq libraries were prepared using Illumina RNA-Seq Preparation Kit and sequenced using a Novaseq 6,000 platform in CCHMC DNA Sequencing and Genotyping Core. Reads were aligned to reference mouse genome mm10 and DESeq2 was used for differential gene expression analysis. EnhancedVolcano R package was used for volcano plot generation and pheatmap R package was used for heatmap generation.

CUT&RUN—The CUT & RUN experiments were performed as previously described (Skene et al., 2018). In briefly, sorted $CD44^+TER119^+$ erythroblast cells were attached to the Concanavalin A-coated magnetic beads and stained with primary antibodies over-night at 4°C. pAMN binding was performed at a final concentration of 700ng/mL and targeted digestion under 100mM CaCl2 at 0°C block. The released DNA was extracted using a Qiagen MinElute kit and libraries were prepared with the NEBNext® Ultra™ II DNA Library Prep Kit for Illumina (#E7645). Barcoded libraries were sequenced using a HiSeq 2,500 sequencer at the DNA core of Cincinnati Children's Hospital Medical Center. The antibodies are listed below: anti-CHD8 (Bethyl Laboratories, # A301–224).

QUANTIFICATION AND STATISTICAL ANALYSIS

Statistical analyses were done using GraphPad Prism software. All data are shown as mean ± s.e.m. Two tailed Student's t test was used to determine statistical significance. Significance was set as * for $p < 0.05$, ** for $p < 0.01$, and ***$p < 0.001$, unless otherwise indicated.

Supplementary Material

Refer to Web version on PubMed Central for supplementary material.

ACKNOWLEDGMENTS

This work was in part supported by NIH grants U54 DK126108, R01 HL147536, and R01 CA234038 and by a grant from CancerFree Kids.

REFERENCES

Amaya M, Desai M, Gnanapragasam MN, Wang SZ, Zu Zhu S, Williams DC Jr., and Ginder GD (2013). Mi2β-mediated silencing of the fetal γ-globin gene in adult erythroid cells. Blood 121, 3493–3501. 10.1182/blood-2012-11-466227. [PubMed: 23444401]

Bernier R, Golzio C, Xiong B, Stessman HA, Coe BP, Penn O, Witherspoon K, Gerdts J, Baker C, Vulto-van Silfhout AT, et al. (2014). Disruptive CHD8 mutations define a subtype of autism early in development. Cell 158, 263–276. 10.1016/j.cell.2014.06.017. [PubMed: 24998929]

Bultman SJ, Gebuhr TC, and Magnuson T (2005). A Brg1 mutation that uncouples ATPase activity from chromatin remodeling reveals an essential role for SWI/SNF-related complexes in beta-globin expression and erythroid development. Genes Dev 19, 2849–2861. 10.1101/gad1364105.. [PubMed: 16287714]

Durak O, Gao F, Kaeser-Woo YJ, Rueda R, Martorell AJ, Nott A, Liu CY, Watson LA, and Tsai LH (2016). Chd8 mediates cortical neurogenesis via transcriptional regulation of cell cycle and Wnt signaling. Nat. Neurosci 19, 1477–1488. 10.1038/nn.4400. [PubMed: 27694995]

Etienne-Manneville S, and Hall A (2002). Rho GTPases in cell biology. Nature 420, 629–635. 10.1038/nature01148. [PubMed: 12478284]

Flanagan JF, Mi LZ, Chruszcz M, Cymborowski M, Clines KL, Kim Y, Minor W, Rastinejad F, and Khorasanizadeh S (2005). Double chromodomains cooperate to recognize the methylated histone H3 tail. Nature 438, 1181–1185. 10.1038/nature04290. [PubMed: 16372014]

Iolascon A, Andolfo I, and Russo R (2020). Congenital dyserythropoietic anemias. Blood 136, 1274–1283. 10.1182/blood.2019000948. [PubMed: 32702750]

Iolascon A, Heimpel H, Wahlin A, and Tamary H (2013). Congenital dyserythropoietic anemias: molecular insights and diagnostic approach. Blood 122, 2162–2166. 10.1182/blood-2013-05-468223. [PubMed: 23940284]

Jaffe AB, and Hall A (2005). Rho GTPases: biochemistry and biology. Annu. Rev. Cell Dev. Biol 21, 247–269. 10.1146/annurev.cellbio.21020604.150721.. [PubMed: 16212495]

Jennings RT, and Knaus UG (2014). Rho family and Rap GTPase activation assays. Methods Mol. Biol 1124, 79–88. 10.1007/978-1-62703-845-4_6. [PubMed: 24504947]

Ji P, Jayapal SR, and Lodish HF (2008). Enucleation of cultured mouse fetal erythroblasts requires Rac GTPases and mDia2. Nat. Cell Biol 10, 314–321. 10.1038/ncb1693. [PubMed: 18264091]

Ji P, Murata-Hori M, and Lodish HF (2011). Formation of mammalian erythrocytes: chromatin condensation and enucleation. Trends Cell Biol 21, 409–415. 10.1016/j.tcb.2011.04.003. [PubMed: 21592797]

Kalfa TA, and Zheng Y (2014). Rho GTPases in erythroid maturation. Curr. Opin. Hematol 21, 165–171. 10.1097/moh.0000000000000032. [PubMed: 24492678]

Katayama Y, Nishiyama M, Shoji H, Ohkawa Y, Kawamura A, Sato T, Suyama M, Takumi T, Miyakawa T, and Nakayama KI (2016). CHD8 haploinsufficiency results in autistic-like phenotypes in mice. Nature 537, 675–679. 10.1038/nature19357. [PubMed: 27602517]

Kawamura A, Katayama Y, Kakegawa W, Ino D, Nishiyama M, Yuzaki M, and Nakayama KI (2021). The autism-associated protein CHD8 is required for cerebellar development and motor function. Cell Rep 35, 108932. 10.1016/j.celrep.2021.108932. [PubMed: 33826902]

Kita Y, Katayama Y, Shiraishi T, Oka T, Sato T, Suyama M, Ohkawa Y, Miyata K, Oike Y, Shirane M, et al. (2018). The autism-related protein CHD8 cooperates with C/EBPβ to regulate adipogenesis. Cell Rep 23, 1988–2000. 10.1016/j.celrep.2018.04.050. [PubMed: 29768199]

Konstantinidis DG, Giger KM, Risinger M, Pushkaran S, Zhou P, Dexheimer P, Yerneni S, Andreassen P, Klingmüller U, Palis J, et al. (2015). Cytokinesis failure in RhoA-deficient mouse erythroblasts involves actomyosin and midbody dysregulation and triggers p53 activation. Blood 126, 1473–1482. 10.1182/blood-2014-12-616169. [PubMed: 26228485]

Konstantinidis DG, Pushkaran S, Johnson JF, Cancelas JA, Manganaris S, Harris CE, Williams DA, Zheng Y, and Kalfa TA (2012). Signaling and cytoskeletal requirements in erythroblast enucleation. Blood 119, 6118–6127. 10.1182/blood-2011-09-379263. [PubMed: 22461493]

Kweon H, Jung WB, Im GH, Ryoo J, Lee JH, Do H, Choi Y, Song YH, Jung H, Park H, et al. (2021). Excitatory neuronal CHD8 in the regulation of neocortical development and sensory-motor behaviors. Cell Rep 34, 108780. 10.1016/j.celrep.2021.108780. [PubMed: 33626347]

Romero-Cortadellas L, Hernández G, Ferrer-Cortès X, Venturi V, Olivella M, Pérez de Soto C, Morales-Camacho RM, Villegas A, Gonzalez-Fernandez FA, Morado M, and Pérez-Montero S (2021). Autosomal recessive congenital dyserythropoietic anemia type iii is caused by mutations in the centralspindlin RACGAP1 component. Blood 138, 847. [PubMed: 33988686]

Liu J, Zhang J, Ginzburg Y, Li H, Xue F, De Franceschi L, Chasis JA, Mohandas N, and An X (2013). Quantitative analysis of murine terminal erythroid differentiation in vivo: novel method to study normal and disordered erythropoiesis. Blood 121, e43–e49. 10.1182/blood-2012-09-456079. [PubMed: 23287863]

Manning BJ, and Yusufzai T (2017). The ATP-dependent chromatin remodeling enzymes CHD6, CHD7, and CHD8 exhibit distinct nucleosome binding and remodeling activities. J. Biol. Chem 292, 11927–11936. 10.1074/jbc.m117.779470. [PubMed: 28533432]

Mei Y, Liu Y, and Ji P (2021). Understanding terminal erythropoiesis: an update on chromatin condensation, enucleation, and reticulocyte maturation. Blood Rev 46, 100740. 10.1016/j.blre.2020.100740. [PubMed: 32798012]

Mei Y, Zhao B, Yang J, Gao J, Wickrema A, Wang D, Chen Y, and Ji P (2016). Ineffective erythropoiesis caused by binucleated late-stage erythroblasts in mDia2 hematopoietic specific knockout mice. Haematologica 101, e1–e5. 10.3324/haematol.2015.134221. [PubMed: 26471482]

Menon V, and Ghaffari S (2021). Erythroid enucleation: a gateway into a “bloody” world. Exp. Hematol 95, 13–22. 10.1016/j.exphem2021.01.001.. [PubMed: 33440185]

Nishiyama M, Oshikawa K, Tsukada Y.i., Nakagawa T, Iemura S.i., Natsume T, Fan Y, Kikuchi A, Skoultchi AI, and Nakayama KI (2009). CHD8 suppresses p53-mediated apoptosis through histone H1 recruitment during early embryogenesis. Nat. Cell Biol 11, 172–182. 10.1038/ncb1831. [PubMed: 19151705]

Nishiyama M, Skoultchi AI, and Nakayama KI (2012). Histone H1 recruitment by CHD8 is essential for suppression of the Wnt-beta-catenin signaling pathway. Mol. Cell Biol 32, 501–512. 10.1128/mcb.06409-11. [PubMed: 22083958]

Nita A, Muto Y, Katayama Y, Matsumoto A, Nishiyama M, and Nakayama KI (2021). The autism-related protein CHD8 contributes to the stemness and differentiation of mouse hematopoietic stem cells. Cell Rep 34, 108688. 10.1016/j.celrep.2021.108688. [PubMed: 33535054]

Pronk CJ, Rossi DJ, Månsson R, Attema JL, Norddahl GL, Chan CKF, Sigvardsson M, Weissman IL, and Bryder D (2007). Elucidation of the phenotypic, functional, and molecular topography of a myeloerythroid progenitor cell hierarchy. Cell Stem Cell 1, 428–442. 10.1016/j.stem.2007.07.005. [PubMed: 18371379]

Rodríguez-Paredes M, Ceballos-Chávez M, Esteller M, García-Domínguez M, and Reyes JC (2009). The chromatin remodeling factor CHD8 interacts with elongating RNA polymerase II and controls expression of the cyclin E2 gene. Nucleic Acids Res 37, 2449–2460. 10.1093/nar/gkp101. [PubMed: 19255092]

Shang X, Marchioni F, Sipes N, Evelyn CR, Jerabek-Willemsen M, Duhr S, Seibel W, Wortman M, and Zheng Y (2012). Rational design of small molecule inhibitors targeting RhoA subfamily Rho GTPases. Chem Biol 19, 699–710. 10.1016/j.chembiol.2012.05.009. [PubMed: 22726684]

Skene PJ, Henikoff JG, and Henikoff S (2018). Targeted in situ genome-wide profiling with high efficiency for low cell numbers. Nat. Protoc 13, 1006–1019. 10.1038/nprot.2018.015. [PubMed: 29651053]

Sood S, Weber CM, Hodges HC, Krokhotin A, Shalizi A, and Crabtree GR (2020). CHD8 dosage regulates transcription in pluripotency and early murine neural differentiation. Proc. Natl. Acad. Sci. USA 117, 22331–22340. 10.1073/pnas.1921963117. [PubMed: 32839322]

Subtil-Rodríguez A, Vázquez-Chávez E, Ceballos-Chávez M, Rodríguez-Paredes M, Martín-Subero JI, Esteller M, and Reyes JC (2014). The chromatin remodeller CHD8 is required for E2F-dependent transcription activation of S-phase genes. Nucleic Acids Res 42, 2185–2196. 10.1093/nar/gkt1161. [PubMed: 24265227]

Thompson BA, Tremblay V, Lin G, and Bochar DA (2008). CHD8 is an ATP-dependent chromatin remodeling factor that regulates beta-catenin target genes. Mol. Cell Biol 28, 3894–3904. 10.1128/mcb.00322-08. [PubMed: 18378692]

Tu Z, Wang C, Davis AK, Hu M, Zhao C, Xin M, Lu QR, and Zheng Y (2021). The chromatin remodeler CHD8 governs hematopoietic stem/progenitor survival by regulating ATM-mediated P53 protein stability. Blood 138, 221–233. 10.1182/blood.2020009997. [PubMed: 34292326]

Ubukawa K, Goto T, Asanuma K, Sasaki Y, Guo YM, Kobayashi I, Sawada K, Wakui H, and Takahashi N (2020). Cdc42 regulates cell polarization and contractile actomyosin rings during terminal differentiation of human erythroblasts. Sci. Rep 10, 11806. 10.1038/s41598-020-68799-1. [PubMed: 32678227]

Watanabe S, De Zan T, Ishizaki T, Yasuda S, Kamijo H, Yamada D, Aoki T, Kiyonari H, Kaneko H, Shimizu R, et al. (2013). Loss of a Rho-regulated actin nucleator, mDia2, impairs cytokinesis during mouse fetal erythropoiesis. Cell Rep 5, 926–932. 10.1016/j.celrep.2013.10.021. [PubMed: 24239357]

Wontakal SN, Britto M, Zhang H, Han Y, Gao C, Tannenbaum S, Durham BH, Lee MT, An X, and Mishima M (2022). RACGAP1 Variants in a Sporadic Case of CDA III Implicates the Dysfunction of Centralspindlin as the Basis of the Disease. Blood 139, 1413–1418. 10.1182/blood.2021012334. [PubMed: 34818416]

Wu J, Krchma K, Lee HJ, Prabhakar S, Wang X, Zhao H, Xing X, Seong RH, Fremont DH, Artyomov MN, et al. (2020). Requisite chromatin remodeling for myeloid and erythroid lineage differentiation from erythromyeloid progenitors. Cell Rep 33, 108395. 10.1016/j.celrep.2020.108395. [PubMed: 33207205]

Yang W, Liu B, Gao R, Snetselaar LG, Strathearn L, and Bao W (2021). Association of anemia with neurodevelopmental disorders in a nationally representative sample of US children. J. Pediatr 228, 183–189.e2. 10.1016/j.jpeds.2020.09.039. [PubMed: 33035572]

Zhao C, Dong C, Frah M, Deng Y, Marie C, Zhang F, Xu L, Ma Z, Dong X, Lin Y, et al. (2018). Dual requirement of CHD8 for chromatin landscape establishment and histone methyltransferase recruitment to promote CNS myelination and repair. Dev. Cell 45, 753–768.e8. 10.1016/j.devcel.2018.05.022. [PubMed: 29920279]

Zhou Y, Zhou B, Pache L, Chang M, Khodabakhshi AH, Tanaseichuk O, Benner C, and Chanda SK (2019). Metascape provides a biologist-oriented resource for the analysis of systems-level datasets. Nat. Commun 10, 1523. 10.1038/s41467-019-09234-6. [PubMed: 30944313]

Author Manuscript
Author Manuscript
Author Manuscript

Highlights

- The autism-related chromatin remodeler CHD8 is essential for erythroid differentiation
- CHD8 controls erythroblast cytokinesis
- Loss of CHD8 causes CDA-like anemia independent of P53 or β-catenin signaling
- CHD8 governs the precise balance of Rho GTPase signaling in erythroblasts

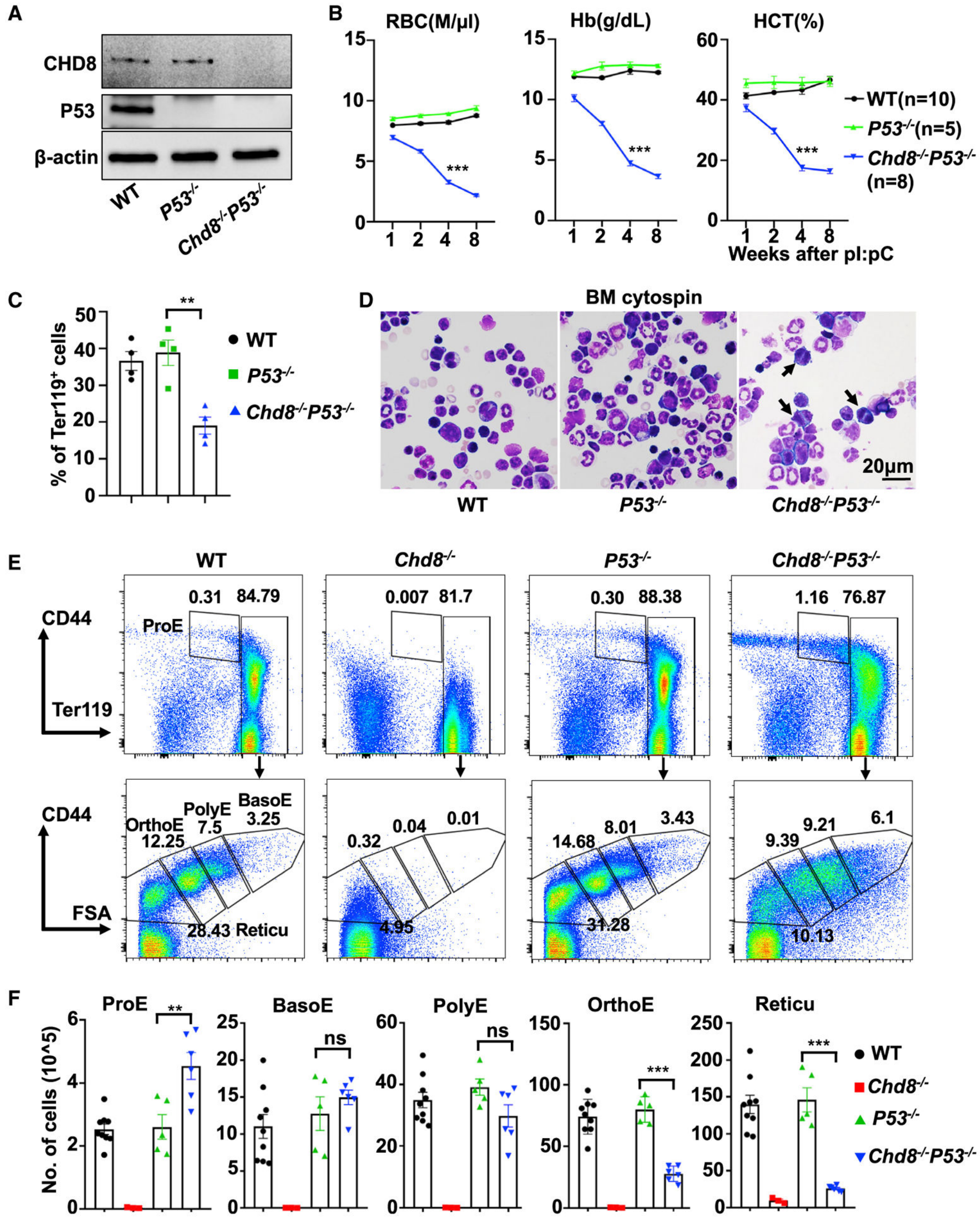

Figure 1. CHD8 is required for erythropoiesis in the BM

(A) Western blots of CHD8 and P53 in *$Chd8^{F/F}P53^{F/F}$*, *$P53^{F/F}$*; *Mx1-Cre* and *$Chd8^{F/F}P53^{F/F}$*; *Mx1-Cre* erythroblast 2 weeks after pI:pC induction.

(B) Peripheral blood counts of RBCs, Hb, and Hct in *$Chd8^{F/F}P53^{F/F}$*, *$P53^{F/F}$*; *Mx1-Cre* and *$Chd8^{F/F}P53^{F/F}$*; *Mx1-Cre* mice after pI:pC induction by Hemavet. The statistics were by t test at 4 weeks post-deletion between *$Chd8^{-/-}$ $P53^{-/-}$* and *$P53^{-/-}$* mice. ***p < 0.001. The x axis indicates the weeks after last pI:pC injection. Biological replicates, n = 10 for WT, 5 for *$P53^{-/-}$*, and 8 for *$Chd8^{-/-}$ $P53^{-/-}$*.

(C) The ratio of TER119^{+} cells in the BM of WT, *$P53^{-/-}$*, and *$Chd8^{-/-}$ $P53^{-/-}$* mice. **p < 0.01. Biological replicates, n = 4 for each genotype.

(D) Cytospin of WT, *P53*$^{-/-}$, and *Chd8*$^{-/-}$ *P53*$^{-/-}$ BM cells. Scale bar, 20 μm. The arrows indicated the bi-nucleated erythroblasts.

(E) Flow cytometry analysis of BM erythroid differentiation with CD44 and TER119 markers in WT, *P53*$^{-/-}$, *Chd8*$^{-/-}$, and *Chd8*$^{-/-}$ *P53*$^{-/-}$ mice. CD45^{-} BM cells were plotted in the top chart, and the numbers in the flow chart are the percentages of parent gating.

(F) Number of erythroblasts at different stages in WT, *P53*$^{-/-}$, *Chd8*$^{-/-}$, and *Chd8*$^{-/-}$ *P53*$^{-/-}$ mice. Student's t test was performed between *Chd8*$^{-/-}$ *P53*$^{-/-}$ and *P53*$^{-/-}$ mice. ***$p < 0.001$, **$p < 0.01$, ns, not significant. Biological replicates, n = 9 for WT, 5 for *P53*$^{-/-}$, and 6 for *Chd8*$^{-/-}$ *P53*$^{-/-}$.

See also Figures S1 and S2.

Author Manuscript
Author Manuscript
Author Manuscript

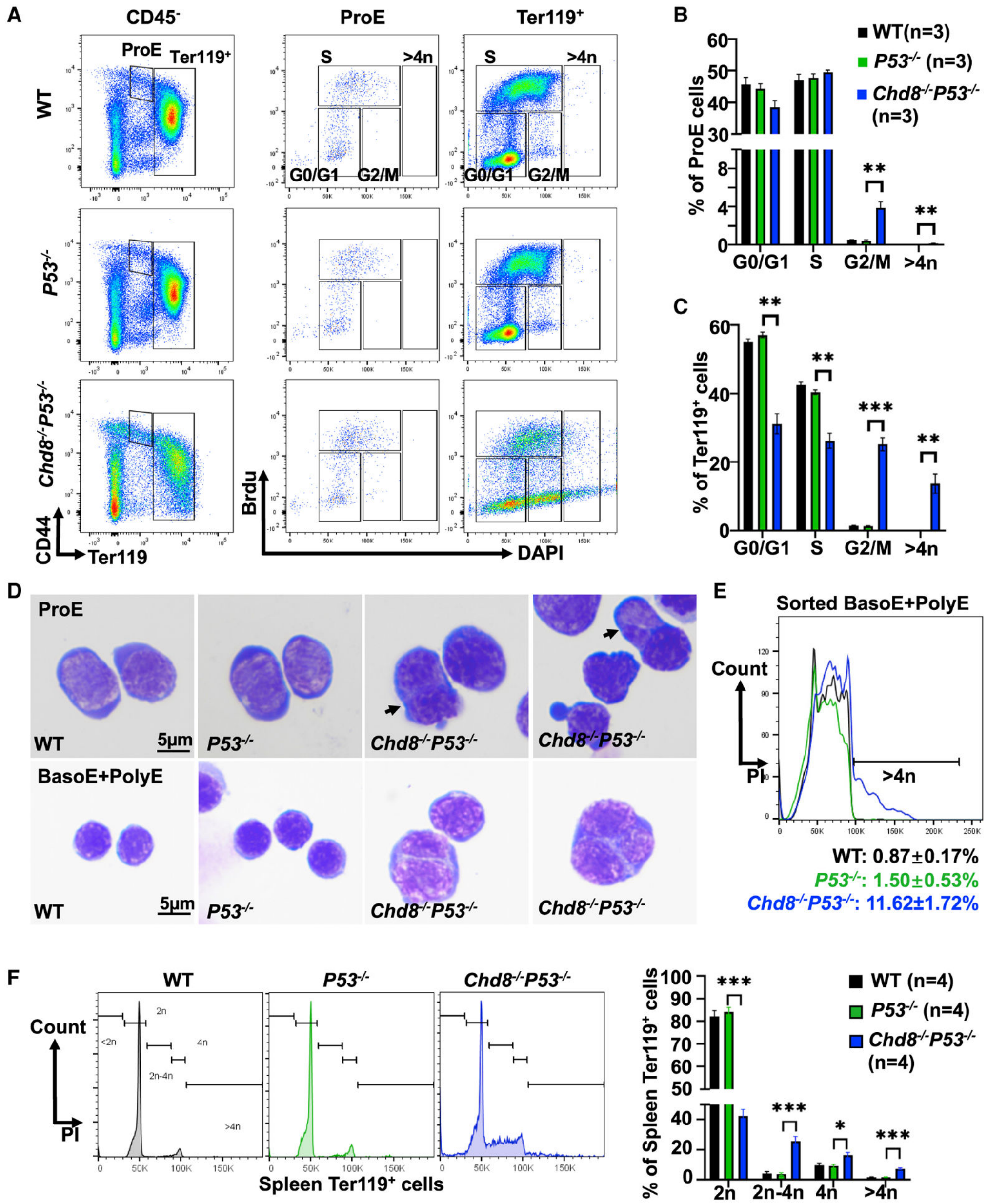

Figure 2. CHD8 is required for erythroblast cytokinesis during erythropoiesis

(A) Representative flow charts of *in vivo* BrdU-labeled erythroid cells from WT, *P53*$^{-/-}$, and *Chd8*$^{-/-}$ *P53*$^{-/-}$ mice at 2 weeks post pI:pC injection.

(B) Percentages of G0/G1, S, G2/M, and >4N cells in ProEs of each genotype. **p < 0.01. Experiments were performed in biological triplicates.

(C) Percentages of G0/G1, S, G2/M, and >4N cells in TER119^{+} population at 2 weeks post deletion. ***p < 0.001, **p < 0.01. Experiments were performed in biological triplicates.

(D) Wright staining images of sorted ProEs and BaosEs + PolyEs for each genotype. Scale bar, 5 μm. Arrow indicated polyploid cells.

(E) PI staining for DNA content in sorted BasoE + PolyE cells at 2 weeks after deletion. The number below represents the mean ± SEM of the percentage of DNA content >4N cells for each genotype. Experiments were performed in biological triplicates.

(F) PI flow cytometry results of spleen TER119^{+} cells, and percentage of cells in different cell-cycle stages. ***p < 0.001, *p < 0.05. Biological replicates, n = 4 for each genotype. See also Figure S3.

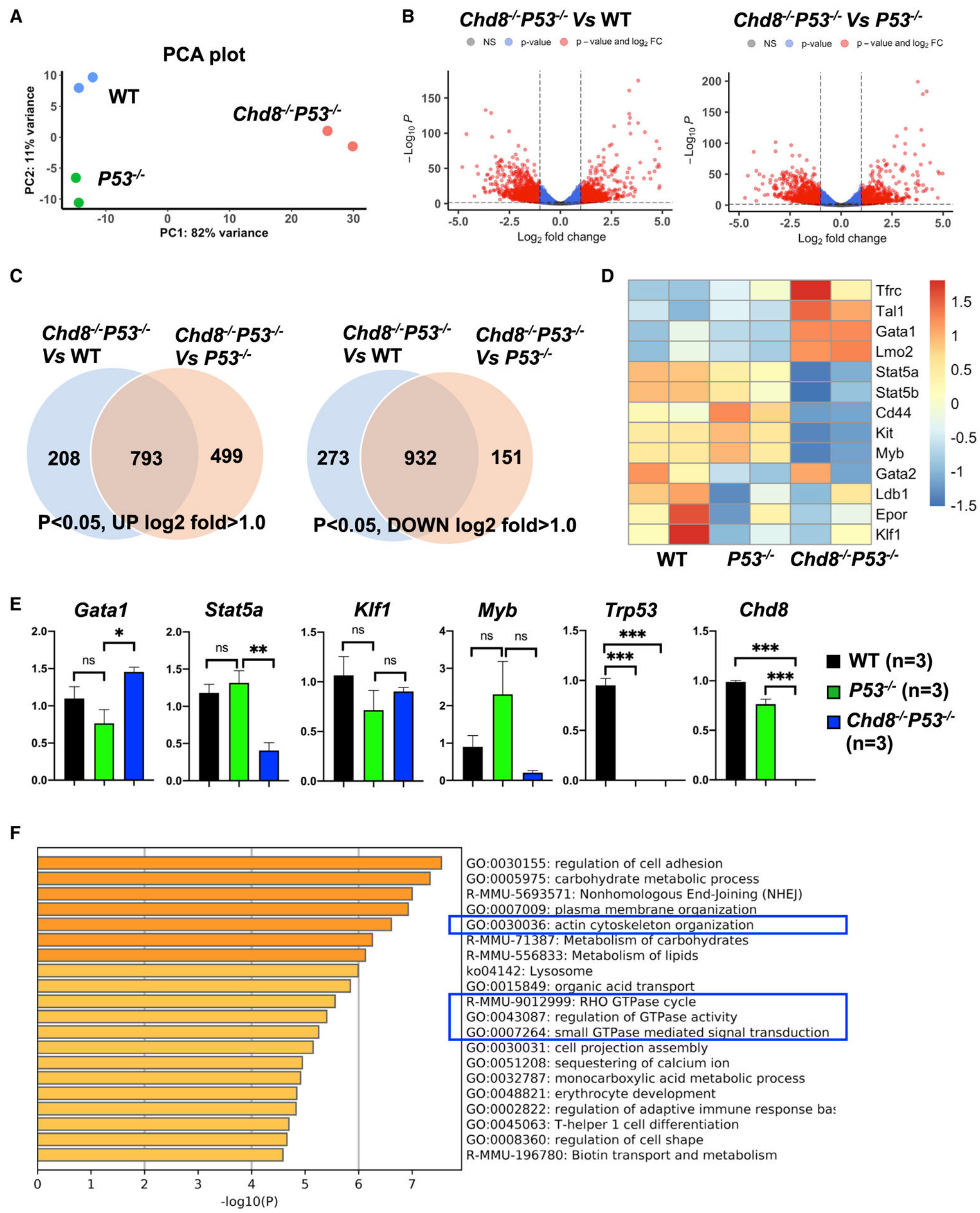

Figure 3. RNA-seq of ProEs identifies gene expression changes in *Chd8*$^{-/-}$ *P53*$^{-/-}$ mice

(A) PCA plot of RNA-seq duplicates for each genotype.

(B) Differentially expressed genes between *Chd8*$^{-/-}$ *P53*$^{-/-}$ and WT and *Chd8*$^{-/-}$ *P53*$^{-/-}$ and *P53*$^{-/-}$. $p < 0.05$. Log2 fold change > 1.0.

(C) Overlapping of differentially expressed genes between *Chd8*$^{-/-}$ *P53*$^{-/-}$ and WT and *Chd8*$^{-/-}$ *P53*$^{-/-}$ and *P53*$^{-/-}$ to find the commonly changed genes in *Chd8*$^{-/-}$ *P53*$^{-/-}$.

(D) Heatmap of key molecules expression in WT, *P53*$^{-/-}$, and *Chd8*$^{-/-}$ *P53*$^{-/-}$ ProE RNA-seq data.

(E) RT-PCR of representative genes in sorted erythroblast cells to confirm the changes observed in RNA-seq data. ***$p < 0.001$, **$p < 0.01$, *$p < 0.05$, ns, not significant. Experiments were performed in biological triplicates with technical duplicates.

(F) GO analysis of commonly changed genes in *Chd8*$^{-/-}$ *P53*$^{-/-}$ compared with WT and *P53*$^{-/-}$ using Metascape website.
See also Figure S4.

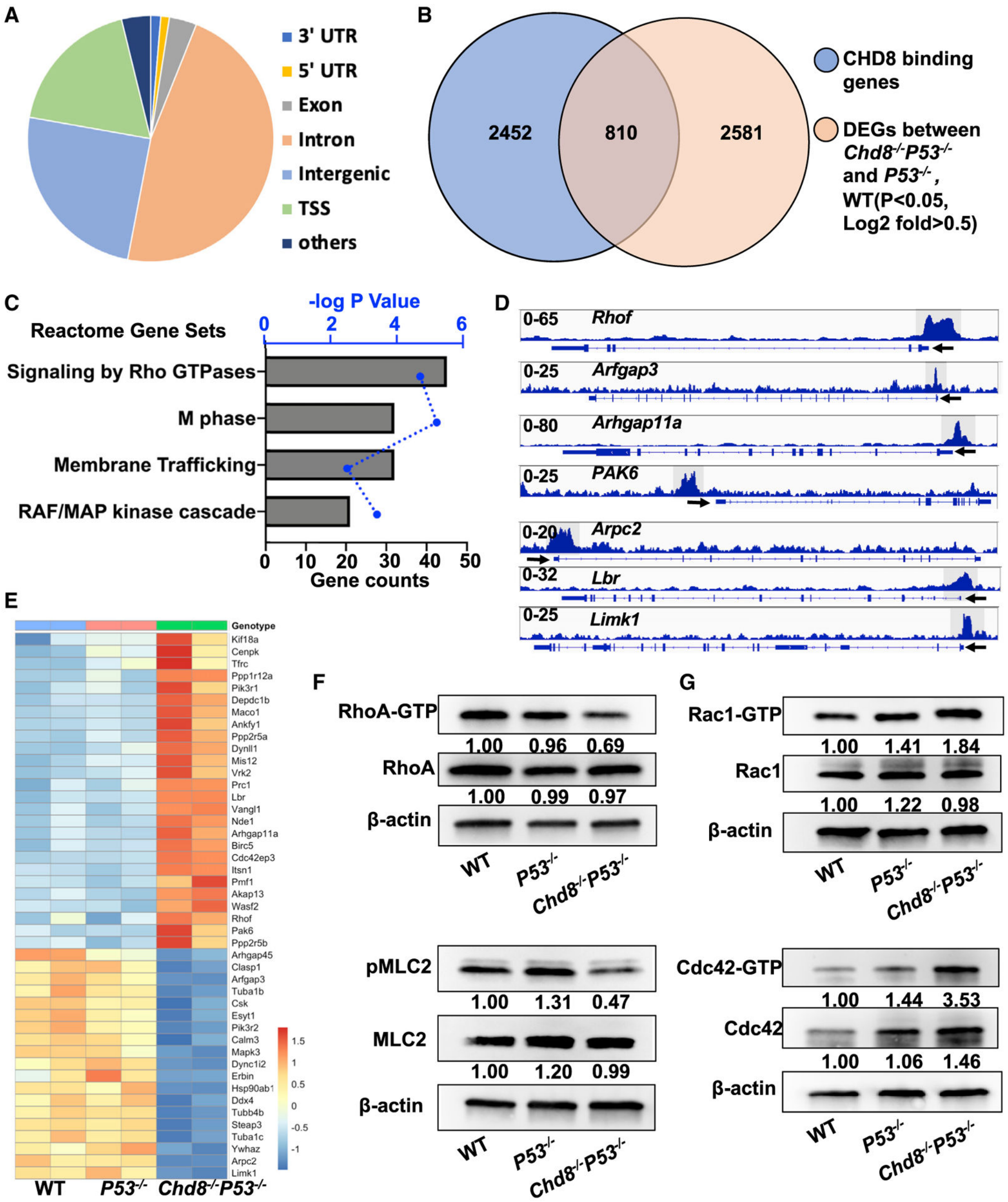

Figure 4. Defective Rho GTPase signaling is involved in cytokinesis failure in *Chd8*$^{-/-}$ *P53*$^{-/-}$ erythroblasts

(A) Location of CHD8 binding peaks in sorted CD44^{+}TER119^{+} cells identified by CHD8 CUT&RUN assay.

(B) Genes overlapping between CHD8 binding targets and differentially expressed genes (DEGs) identified in *Chd8*$^{-/-}$ *P53*$^{-/-}$ cells through RNA-seq.

(C) Reactome gene set enrichment with the differentially expressed CHD8 direct targets by Metascape website.

(D) Representative CHD8 Cut & Run tracks of *Rhof*, *Arfgap3*, *Arhgap11a*, *Pak6*, *Lbr*, *Limk1*, and *Arpc2* in WT erythroblasts generated by IGV software.

(E) Expression heatmap of CHD8 target genes enriched in signaling by Rho GTPases in RNA-seq data.

(F) RhoA-GTP level detected by pull-down assays with Rhotekin beads and western blotting (WB) of pMLC2 Ser19 and MLC2 in CD45^{-}TER119^{+} BM cells of WT, *P53*$^{-/-}$, and *Chd8*$^{-/-}$ *P53*$^{-/-}$ mice.

(G) Rac1-GTP and Cdc42-GTP levels in each genotype detected by pull-down assays with PAK beads in CD45^{-}TER119^{+} BM cells.

In (F) and (G), the number indicates the mean intensity level derived from 2 independent experiments. Protein levels were normalized to β-actin with levels in WT cells arbitrarily set at 1. Each experiment includes 3 mice for each genotype, and TER119^{+} cells were pulled together and used for protein extraction.

KEY RESOURCES TABLE

REAGENT or RESOURCE	SOURCE	IDENTIFIER
Antibodies		
APC anti-mouse CD45	Biolegend	Cat# 103,111; RRID:AB_312976
FITC anti-mouse TER119 antibody	Biolegend	Cat# 116,206; RRID:AB_313707
PerCP/Cy5.5 anti-mouse Ly-6A/E (Sca-1)	Biolegend	Cat# 108124; RRID:AB_893615
APC/Cyanine7 anti-mouse CD117	Biolegend	Cat# 105826; RRID:AB_1626278
PE anti-mouse CD41 antibody	Biolegend	Cat# 133906; RRID:AB_2129745
PE/Cy7 anti-mouse CD150	Biolegend	Cat# 115914; RRID:AB_439797
FITC anti-mouse CD16/32 antibody	Biolegend	Cat# 101305; RRID:AB_312804
APC anti-mouse CD105 antibody	Biolegend	Cat# 120414; RRID:AB_2277914
PE anti-mouse/human CD44	Biolegend	Cat# 103008; RRID:AB_312959
PE anti-mouse CD71 antibody	Biolegend	Cat# 113807; RRID:AB_313568
PerCP/Cy5.5 anti-mouse TER-119	Biolegend	Cat# 116228; RRID:AB_893636
Rabbit anti-CHD8 Antibody	Bethyl	Cat# A301–224A; RRID:AB_890578
RhoA (67B9) Rabbit mAb antibody	Cell Signaling Technology	Cat# 2117; RRID:AB_10693922
Anti-Rac1, clone 23A8 antibody	Millipore	Cat# 05–389; RRID:AB_309712
Cdc42 (11A11) Rabbit mAb antibody	Cell Signaling Technology	Cat# 2466; RRID:AB_2078082
Phospho-Myosin Light Chain 2 (Ser19) Antibody	Cell Signaling Technology	Cat# 3671; RRID:AB_330248
Myosin Light Chain 2 (D18E2) antibody	Cell Signaling Technology	Cat# 8505; RRID:AB_2728760
Chemicals, peptides, and recombinant proteins		
4’,6 Diamidino 2 Phenylindole, Dihydrochloride	Thermo Fisher Scientific	Cat# D1306
Propidium Iodide Solution	BioLegend	Cat# 421301
Methylcellulose-based medium with EPO (without other cytokines) for mouse cells	STEMCELL Technologies	Cat # 03334
Serum-free methylcellulose-based medium with recombinant cytokines (including EPO) for mouse erythroid progenitor cells	STEMCELL Technologies	Cat # 03436
Harleco® Hematology Stains and Reagents	Sigma-Aldrich	Cat # 740–75
Critical commercial assays		
FITC BrdU Flow Kit	BD Biosciences	Cat # 559619
FITC Annexin V 100 tests	BioLegend	Cat # 640906
Mouse Erythropoietin ELISA Kit	Abcam	Cat # ab270893
Camco Stain Pak-3 bottle stain kit	Cambridge Diagnostic Products	Cat # 702
CUT&RUN Assay Kit	Cell Signaling Technology	Cat # 86652S
NEBNext Ultra II DNA Library Prep with Sample Purification Beads	New England Biolabs (NEB)	Cat # E7103S
NEBNext® Multiplex Oligos for Illumina® (Index Primers Set 4)	New England Biolabs (NEB)	Cat # E7730S
Miltenyi Biotec, Inc. CD45 MICROBEADS	Miltenyi Biotec	Cat # 130-052-301
Miltenyi Biotec, Inc. TER 119 MICRO BEADS MOUSE	Miltenyi Biotec	Cat #130-049-901
Deposited data		
ProE RNA sequencing	This paper	GSE: GSE189853

REAGENT or RESOURCE	SOURCE	IDENTIFIER
CHD8 CUT&RUN sequencing data	This paper	GSE: GSE189853
Experimental models: Organisms/strains		
Chd8$^{F/F}$ mice	Q. Richard Lu lab	Zhao et al., 2018
Trp53$^{F/F}$ mice	THE JACKSON LABORATORY	Cat # 008462
Mx1-Cre mice	Yi Zheng lab	N/A
Oligonucleotides		
Primers for Real-time PCR, see Table S1	This paper	N/A
Software and algorithms		
GraphPad Prism 8.4.0	GraphPad	https://www.graphpad.com/
FlowJo V10	BD (Becton, Dickinson & Company)	https://www.flowjo.com/bd-flowjo-faq
FACS Diva	BD Biosciences	https://www.bdbiosciences.com/en-it/products/software/instrument-software/bd-facsdiva-software
DESeq2	Bioconductor	https://doi.org/10.18129/B9.bioc.DESeq2
EnhancedVolcano R package	Bioconductor	https://doi.org/10.18129/B9.bioc.EnhancedVolcano
pheatmap R package	RDocumentation	https://rdocumentation.org/packages/pheatmap/versions/1.0.12
Metascape web tools	Zhou et al., 2019	https://metascape.org/gp/index.html#/main/step1
SEACR 1.4.R	Meers, MP, Tenenbaum, D and Henikoff S (2019)	https://seacr.fredhutch.org/
IGV 2.8.2	Helga Thorvaldsdóttir, James T. Robinson, Jill P. Mesirov. (2013)	https://igv.org/
Image Lab software	Bio Rad	https://www.bio-rad.com/zh-cn/product/image-lab-software?ID=KRE6P5E8Z